Research Article

Journal of Molecular Recognition

Received: 29 November 2013, Revised: 31 March 2014, Accepted: 9 April 2014, Published online in Wiley Online Library

(wileyonlinelibrary.com) DOI: 10.1002/jmr.2381

Application of OmpF nanochannel forming protein in polynucleotide sequence recognition

Saeid Hadi-Alijanvand[a], Hamid Mobasheri[a,b]* and Hamid Hadi-Alijanvand[c]

Recognition of the sequence of human genome sequence is vital to address malfunctions occurring at molecular, cellular and tissue levels and requires a great deal of time, cost and efforts. Thus, various synthetic and natural pores were considered to fabricate high-throughput systems capable to fulfill the task in an efficient manner. Here, voltage gating OmpF nanochannel, whose structure is known at an atomic level, was used to recognize and differentiate between polynucleotide primers through voltage clamp technique. Our results showed that poly(T) occasionally blocked the channel at both polarities, while poly(C) and poly(G) obstructed it only at positive polarity. The channel was blocked at potential differences of as low as 80 mV in the presence of poly(T). The conductance of channel decreased in the presence of poly (C) and poly(G) by 61 and 5% respectively. Analysis of the number of events showed that poly(T) caused more closing events at higher voltages, while poly(G) and poly(C) induced it at lower voltages. Application of the hazard function as a statistical parameter and analysis of event closing times in various voltages demonstrated the most efficient differentiation at 60 mV. The results of practical and theoretical approaches presented here show that OmpF porin channel possesses the structural and dynamic characteristics required to be considered as a biosensor capable for continuous polynucleotide sequencing. Copyright © 2014 John Wiley & Sons, Ltd.

Keywords: biophysics; ion channel; nucleotide sequencing; artificial membrane; voltage clamp

INTRODUCTION

Biological (Butler *et al*., 2008; Purnell and Schmidt, 2009; Stoddart *et al*., 2009; Derrington *et al*., 2010; Stoddart *et al*., 2010; Franceschini *et al*., 2012; Wang *et al*., 2013) and solid-state (Li *et al*., 2001; Binquan *et al*., 2010; Mussi *et al*., 2010; Luan *et al*., 2011; Laun *et al*., 2012) nanopores have shown promising results in probing single molecules in real time. There have been several approaches considered to ease and speed up nucleotide sequencing of DNA and RNA molecules (Venkatesan and Bashir, 2010). Kasianowicz and his colleagues used α-hemolysin (α-HL), from *Staphylococcus aureus* to monitor the effect of single-strand DNA on channel conductivity and current patterns (Kasianowicz *et al*., 1996). Synthetic nanopores have also been used for DNA sequencing and presented several advantages. Li *et al*. demonstrated the formation of synthetic Si3N4 nanopores from thin insulating solid-state membranes using highly focused low-energy ion beams (Li *et al*., 2001), while others sculpted nanopores by electron beams (Storm *et al*., 2003; Heng *et al*., 2004). Si3N4 pore was also used by Heng *et al*. to discriminate between single-stranded and double-stranded DNA molecules, from which the latter was unable to translocate through the pore (Heng *et al*., 2004). Iqbal *et al*. manufactured a solid-state nanopore containing a probe of hairpin loop DNA, able to selectively transport short segments of single-stranded DNA across the pore (Iqbal *et al*., 2007). Most recently, Merchant *et al*. sculpted nanopores with a diameter of as low as 5 nm in 1–5 nm thick graphene membranes by electron beam. Graphene is an electrical conductor, thus, electronic sensing can be performed directly at the pore area (Merchant *et al*., 2010).

Nanochannel forming proteins were also used to study the translocation of both charged hydrophilic as well as neutral molecules. The presence of obstructing molecule in the vestibule/lumen of the channel affects on the flux of current carriers and creates a unique conductive pattern at different membrane potential differences (PDs). The pattern is considered as a signature for each translocating molecule representing the effects of its size, charge, geometry and hydration state (Meni, 2012).

OmpF porin channel

OmpF porin is the first channel forming membrane protein whose structure is known at atomic level (Garavito and Rosenbusch, 1980). The channel is consisted of three homologous identical monomers forming a trimer in the outer membrane of *E. coli*. Each monomer is a beta barrel formed by 16 beta strands connected to each other by eight external loops and eight internal turns. The channel lumen is constricted by L3 loop that folds into the channel

* *Correspondence to: Hamid Mobasheri, Laboratory of Membrane Biophysics and Macromolecules, Institute of Biochemistry and Biophysics, University of Tehran, P.O. Box 13145-1384, Tehran, Iran.*
E-mail: h.mobasheri@ibb.ut.ac.ir

a *S. Hadi-Alijanvand, H. Mobasheri*
Laboratory of Membrane Biophysics and Macromolecules, Institute of Biochemistry and Biophysics, University of Tehran, P.O. Box 13145-1384, Tehran, Iran

b *H. Mobasheri*
Biomaterials Research Center (BRC), University of Tehran, 178, Taleghani Ave., Tehran, Iran

c *H. Hadi-Alijanvand*
Department of Biological Sciences, Institute for Advanced Studies in Basic Sciences (IASBS), P. O. Box 45195-1159, Zanjan, Iran

lumen, forms eyelet area at the mid height of the channel and stabilizes it (Marquis and Ficht, 1993). The cross sectional electric field at this area is formed by an arrangement of negative amino acids, D113 and E117, on the L3 that point toward positively charged amino acids, R42, R82 and R132, located on the channel barrel wall (Karshikoff *et al*., 1994). As a result, electrostatic interactions take place (Cowan *et al*., 1992), and cations are selectivity conducted over anions. The structure of wild-type OmpF is quite stable in harsh condition so that it stands temperatures as high as 75°C, acid pH, and bile salts and proteolitic enzymes (Schirmer, 1998) and is similar to other known porins, like PhoE and OmpC (Nikaido, 2003).

Gating mechanisms

Different gating mechanisms have been proposed for OmpF channel, including the following: (i) movement of L3 (Soares *et al*., 1995); (ii) electrostatic interaction with leaning charged groups (Van Gelder *et al*., 1997); (iii) sliding in beta barrel strands (Bainbridge *et al*., 1998); (iv) global folding and refolding of the whole molecule (Müller and Engel, 1999); (v) intermonomers role of lipopolysaccharides(Wiese *et al*., 1994); (vi) lateral pressure and thickness effect of the membrane; (vii) membrane PD(Hille, 1978); (viii) polyamine interaction with the lumen (Ramkumar and Delcour, 1997); and so on (Robertson and Tieleman, 2002). Thus, the actual mechanism involved in voltage-dependent gating in OmpF and OmpC porins is still unknown.

Translocation

Analysis of the movement of inert globular molecules, polyethylene glycols through the channel, has partially revealed the translocation mechanism (Rostovtseva *et al*., 2002a). Voltage-dependent mitochondrial channel has been studied by Rostovtseva and her colleagues (Rostovtseva *et al*., 2002b). The influx of the known antibiotics through OmpF channel has been shown experimentally (Nestorovich *et al*., 2002; Danelon *et al*., 2006; Mach *et al*., 2008; Masi and Pagès, 2013). On the other hand, movement of objects with different sizes through the channel lumen has been approved by theoretical and virtual approaches (Karshikoff *et al*., 1994). The mechanism of translocation of nucleotide through nucleotide interaction with PorB porin that has similar structure to other outer membrane porins was investigated by Tanabe and colleagues (Tanabe *et al*., 2010). Meyer and colleagues proposed OmpF as a novel receptor for translocation of bacteriophage λ genome into *E. coli* (Meyer *et al*., 2012).

Having had the structure of the channel known at the atomic level, it became possible to address the local interaction of the transferring molecule with the channel lining amino acid side chains. Thus, the hydrogen bonds, ionic interactions and the affinity for certain molecules can be worked out by docking programs. Furthermore, the physicochemical condition in the nanoenvironment of the channel lumen caused by deliberate changes in the pH and PDs can be easily addressed (Ramkumar and Delcour, 1997). Further to the structural approaches, it is also possible to conduct real time studies of the dynamic and activity of single channel in artificial bilayers in the presence and absence of the translocating molecule (Nestorovich *et al*., 2003). Some channel forming proteins have been engineered through replacement of certain amino acids by site-directed mutagenesis, and their activity has been studied by voltage clamp studies (Van Gelder *et al*., 1997) and made it possible to understand the channel behavior and to ease the translocation of different molecules.

Having the human complete genome sequence known, it seems that the treatment of certain diseases caused by corrupted gene expression in people with different race, age and so on still requires knowing the individual's genome. This necessitates a dramatic change in current sequencing techniques, and much faster, more efficient and less expensive approaches are required. To fulfill this task, different groups are using synthetic and natural nanopores to construct automated fast and cheap sequencing means. This is why working with α-HL (Kasianowicz *et al*., 1996) and synthetic pores like SiN membranes (Luan *et al*., 2011) has already been started and seems promising. Here, for the first time, we have used OmpF porin as a translocating path for single-strand DNA decamers and have tried to distinguish between different polynucleotides by biophysical aspects involved at single molecule level. This information together with the classic known pattern of the channel conductivity patterns at different physicochemical conditions as well as modeling approaches might pave the path to monitor and characterize the DNA and RNA molecules in real time and in faster, cheaper and more efficient way.

MATERIALS AND METHODS

All experiments were conducted on OmpF porins from *E. coli* K12 purified in our group as well as those kindly provided by Prof. Witterhalter and Dr. Weingart, Jacobs University, Bremen, Germany. All experiments were carried out in 4-(2-hydroxyethyl)-1-piperazineethanesulfonic acid (HEPES) buffer (KCl 1 M, $CaCl_2$ 10 mM, HEPES 10 mM, pH 7.4) at 22°C. Chemicals were received from Sigma Chemicals Co. unless otherwise indicated. DNA primers, poly(T), poly(C) and poly(G) each made of 10 nucleotides, with OD = 12 were purchased from Biomed, Germany. The polynucleotides were diluted in TEA buffer before applying at a final concentration of 0.5 nM. The artificial planar bilayer was formed by Soy Bean lecithin type II, (SIGMA) based on Montal and Mueller technique (Montal and Mueller, 1972).

Single-channel studies were conducted by voltage clamp technique, where the membrane capacitance and integrity was studied by 120-Hz square waves prior to each experiment. The signal was initially produced by a signal generator with an amplitude of 2 Vpp but dropped to 20 mVpp before it was applied to the bilayer. The channel gating pattern and conductance were studied at various membrane PDs (±0–200 mV) applied to the *cis* side with respect to *trans* side that acted as the virtual ground of the electronic system. The signal-to-noise ratio (S/N) was increased by a preamplifier acting as headstage with a gain of up to 10X. Data acquisition was carried out after dual amplification of up to 100 times and filtering by dual low pass filters at about 10 KHz (Adimi Filter Amplifier). The recordings were carried out at 500-μs sampling intervals using Pat 6 and Pat 7 provided by J Dempster, University of Stratchlyde, UK, and were digitized by CED 1401plus, Cambridge, UK. The channel activity was recorded in a Metal Faraday cage (25 × 25 × 35 cm) installed on air table to eliminate electromagnetic field and mechanical vibration noises of the working place. The preamplifier was electrically isolated from main and ran with two 12-V, 35-Amp dry car batteries. Every part of the system was grounded by means of connection to a 4-m copper rod buried in a 6-m well as the earth source. All experiments were repeated at least three times.

The accessible free surfaces of both channel lining amino acid side chains and introduced polynucleotides were calculated based on Born radius of consisted groups. To fulfill this task, a

surrounding polygonal structure was defined around each nucleotide at each frame based on Shoelace equation (Zhang *et al*., 2005), and the binding and interaction sites along with the channel lumen were identified using Slither software (Lee *et al*., 2009). Slither algorithm was used to conduct iterative docking analysis for producing the profile of translocation path through the lumen. The potential energy of ligand–protein interaction, which includes Van der Waals interactions, hydrogen bond, and electrostatic interactions and represents dehydration free energy, was computed by Slither protocol adopted from Autodock4. The geometry and accessibility of the groups located in the constriction zone were considered as a reference. The type of interactions and their statistics were determined by the LIGPLOT program. Accordingly, the 3D maps of interactions were converted to a 2D map for precise interpretations. The binding affinity of nucleotides along with protein lumen was estimated and used to define local binding affinity by using the common relation, $\Delta G = -RT\ln(K)$. ($\Delta G = Gn - Gn - 1$, $Kn = \exp(-\Delta G/RT)$, and $T = 298$ K). Where, Kn represents the affinity of nucleotide to the *n*th lumen binding site with respect to $n - 1$th binding site as the reference state.

RESULTS

The membrane stability was approved by applying of up to ±180 mV in the absence of nucleotides, and no changes in the permeability and capacitance of bilayer were identified. The polynucleotides that were solely introduced to the *cis* side did not form any Donnan potential because of their very low concentration. This was approved during the course of experiment because of the lack of any shift monitored in the level of current baseline in the absence of the applied PD. The channel gating started at PDs as low as ±40 mV (Figure 1), monomeric closure initiated at about ±130 mV, and complete closure occurred at ±180 mV (Figure 5). The conductance of each monomer was 1300 ± 150 pS at both polarities. Substates of about half the size of monomer and fast flickering were distinguished occasionally. In general, channels showed typical activities and characteristics similar to those reported by other groups (Baslé *et al*., 2004).

Effects of polynucleotides on lipid bilayer permeability and stability

Introduction of polynucleotides strands (0.5 nM) to the *cis* side caused no significant effects on bilayer permeability at different voltages after 30-min incubation. The membrane retained its stability, and no significant changes in its capacitance (80 pF) were observed.

The effects of polynucleotides on OmpF channel gating

Introduction of polynucleotides with a final concentration of 0.5 nM to the *cis* side changed the channel activity mainly by causing gating at high frequency at PDs lower than ±100 mV (Figure 1). The frequency of channel gating in the presence of poly(C) mainly increased as the negative PDs applied to the *trans* side (Figure 1). There were less gating occurred at positive polarities, and their amplitude did not increase as such when PDs were increased. Only one of monomers was gating at a time, and no simultaneous dimeric or trimeric gating was monitored (Figure 1). Application of poly(G) caused channel gating and fast flickering at both polarities but was mainly dominant at negative polarities. The frequency of gating was very high, and fast flickering was occurring mainly at higher PDs. Although the major gating at high frequency occurred at high negative PDs, −80 mV, there were occasions where fast flickering monitored at positive polarity too (Figure 1). While in the early stages of introduction of poly(T), no gating caused at both polarities, gradual gating was monitored later on when −ve pd applied (Figure 1). Fast flickering mainly occurred at negative PDs; however, there were occasions, in particular at higher PDs, when it occurred at positive polarities too. Applying the PDs for 30 min caused fast flickering at −80 mV and led to complete closure of the channel. An increase in the gating frequency was only identified at −60 mV, and there was none at +60 mV even after 30 min. Fast flickering was mainly monitored at −40 mV, although there was some at +ve polarity too. Gating at high frequency in the presence of poly(T) at 20 mV only occurred at positive polarities. The open probability of the channel was completely affected by poly(T) so that there were occasions when one, two and even all three monomers were closed at PDs as low as ±80 mV. There was no long-lasting substrate identified in the presence of poly(T).

Effects of polynucleotides on channel conductance

The main conductance of whole OmpF trimer in the control condition in the absence of polynucleotides was about 4500 pS and independent of the applied PDs (Figure 2). The measured conductance of main states in each monomer was consistent with the value published by other groups (Im and Roux, 2002) and represented a linear Ohmic current–voltage relationship. The channels produced both main states, reported by others, as well as transitional intermediate substrates because of their well accommodated and dynamic status in the bilayer (Figure 5). Because of the voltage sensitivity of the channel, it tended to close directly or through several main and/or intermediate substrates at PDs higher than ±170 mV. Introduction of poly(C) into chamber decreased the conductance of the channel to about 3425 ± 70 pS at both polarities. However, there were occasions, at 80 mV, when the conductance of the channel reduced to 3200 pS at positive polarities and to 3360 and 1750 pS at negative polarities. The channel showed a conductance of 3420 and 3380 pS in the presence of polynucleotides in positive and negative polarities at 60 mV, respectively. The channel was blocked in the presence of poly(C) and showed conductance values of about 3660 and 3480 pS at positive and negative polarities at 40 mV, representing a reduction of about 1100 and 1400 pS. A stable conductance of 1850 pS was monitored at positive polarity that lasts for several seconds. The conductance of the channel at 20 mV was 4500 pS at positive polarity and 3380 and 3500 pS at negative polarities. Thus, the higher the PDs applied, the higher was the decline in the channel conductance in the presence of poly(C) (Figure 2). Application of poly(G) caused a significant effect on the channel conductance at 20 mV and represented the conductance values of 3300 and 2960 pS at positive polarities and 2890 and 2000 pS at negative polarities. There were more conductance levels monitored at negative than positive polarities, where rare gatings occurred. The presence of poly(T) caused conductance of about 410 and 2980 pS at −80 mV and 1400 pS at +80 mV, respectively. The conductance of the channel in the presence of poly(T) was about 1500 and 370 pS at +60 mV and 1500 pS at −60 mV (Figure 2). The channel at +40 mV showed a conductance of about 3000 pS, while at −40 mV represented 2700 and 1200 pS, showing a reduction of about 80% for each monomer. The conductance of the channel at 20 mV decreased by about 70%, reaching 2660 pS at +20 mV and 3200 and 1100 pS at −20 mV.

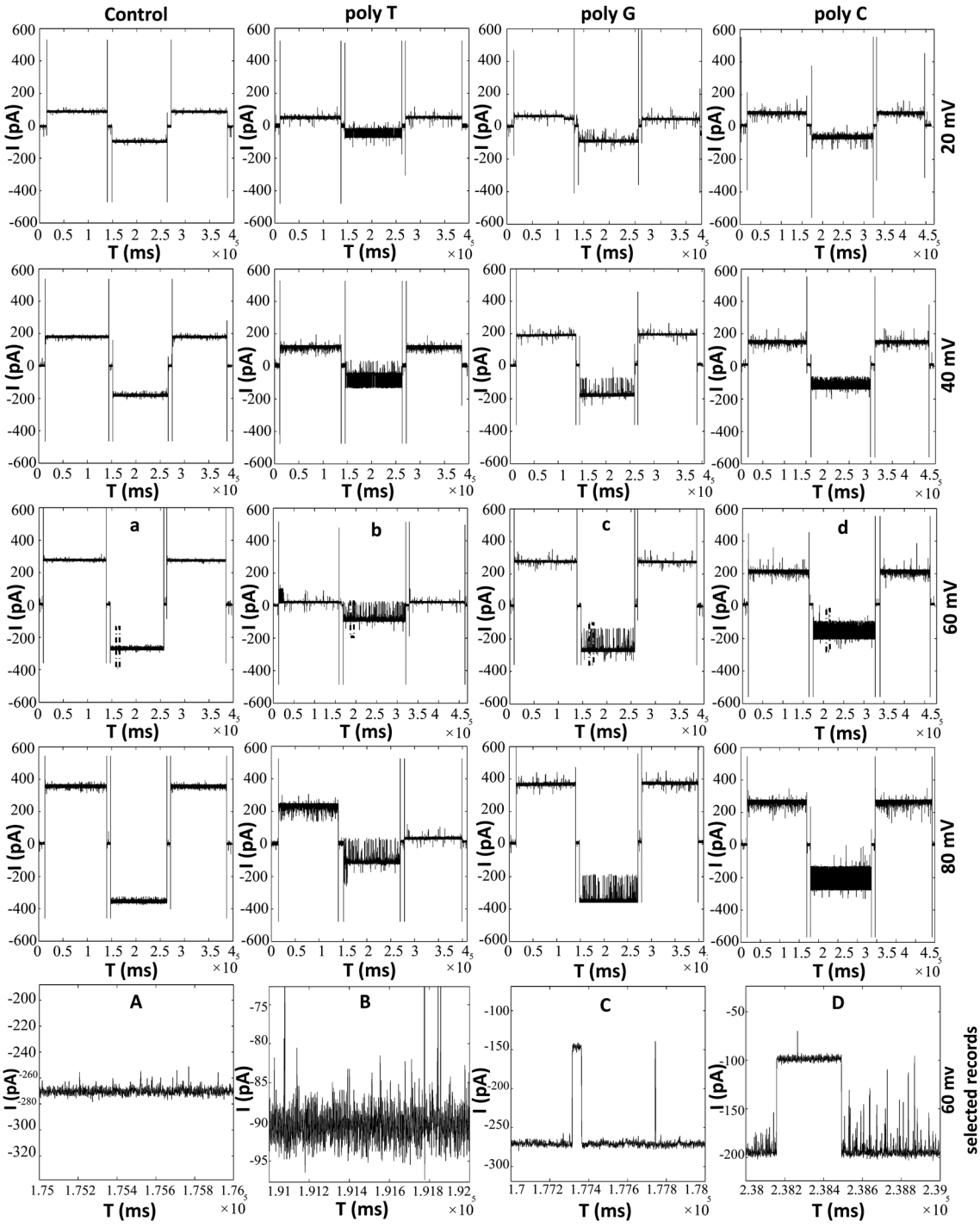

Figure 1. OmpF channel gating in the presence of poly(T), poly(G) and poly(C), at different applied PDs. The higher PDs mainly with negative polarities on the *trans* side caused more gatings. In the presence of poly(T), the gatings initiated at PDs as low as 20 mV and increased at high PDs. There was rarely gating identified in the presence of poly(G) at +ve polarities. In the presence of poly(C), some gating monitored at +ve polarities that were increased at higher PDs; however, significant gating occurred at negative polarities. The boxes shown on the traces at 60 mV in all four groups represent parts that have been magnified and shown in the bottom row. Fast flickering in the presence of poly(T) and partial blockage with different time length in the presence of poly(G) and poly(C) are shown.

Effects of polynucleotides on the number of events in OmpF channel

Analysis of the recorded current traces showed that in the presence of poly(T), the number of events increased as the voltage decreased, while the opposite pattern monitored when poly(C) and poly(G) were introduced (Figure 1). The channel spent various lengths of time at open and closed time in the presence of different polynucleotides. The time length of each closed event represented length of time that each polynucleotide spent to pass

Journal of Molecular Recognition

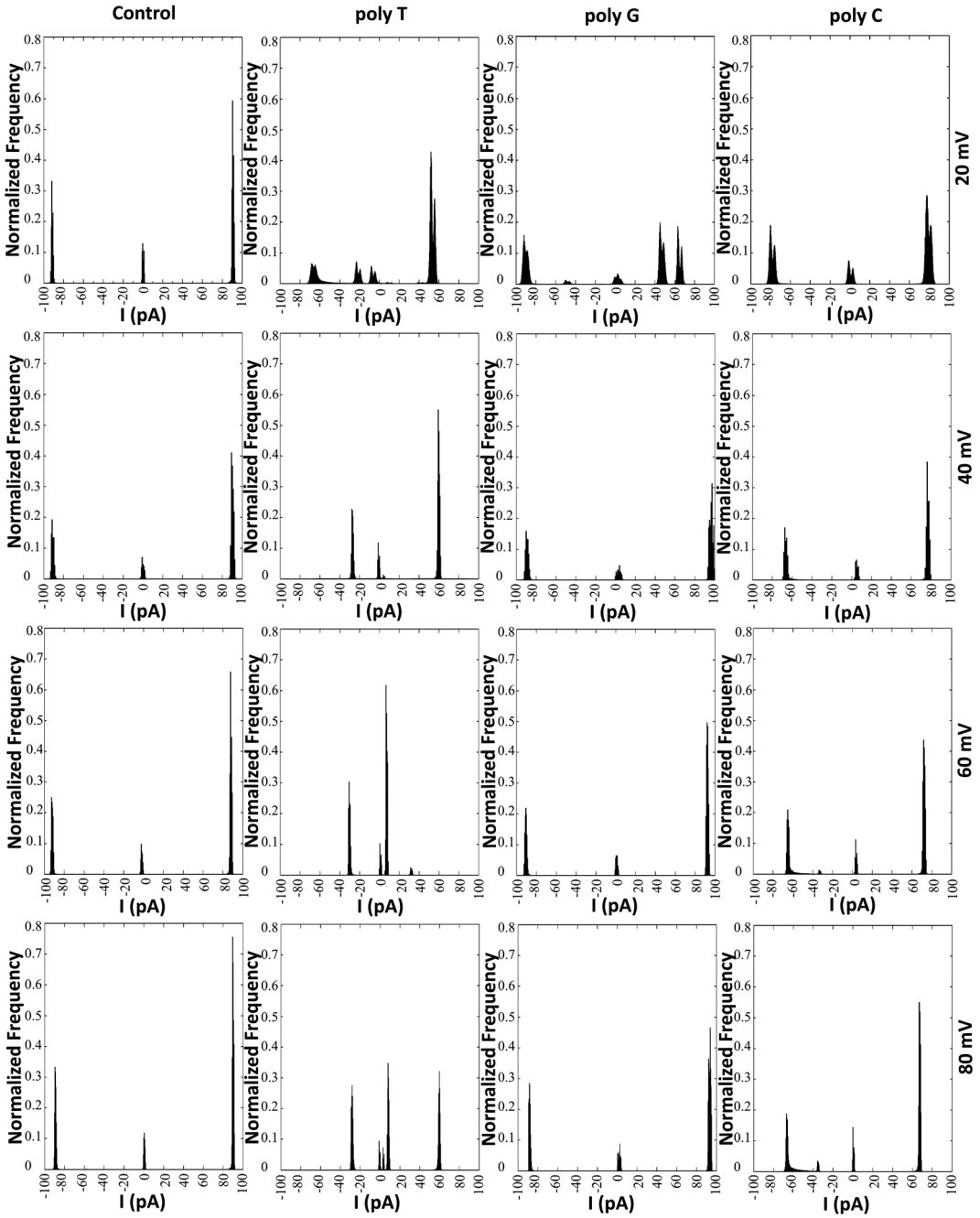

Figure 2. Effects of polynucleotides on current flux through different monomers of the channel 30 min after injection of 0.5 nM of polynucleotides to the *cis* side. The current level in control group shows full open states in all three monomers at ±20–80 mV. In the presence of poly(T), different monomers are obstructed, and current flux at the level of monomer and dimers is produced. In some cases, the channel is nearly blocked by the translocating poly(T). The blockage for poly(G) mainly happened at low PD. Presence of poly(C) caused partial blockage of all monomers causing slight reduction in overall current passing through the channel but did not lead to obstruction.

through the constriction zone of the channel and was manifested by ion current fluctuation. The hazard analysis shows the probability of having long time close states. According to hazard analysis, the channel spent shorter time at closed state in the presence of poly(C), even at PDs as low as 20 to 80 mV that it normally stays in the fully open state. However, in the presence of poly(T), the trend was opposite to that of poly(C) (Figure 3a). Thus, at PDs higher than 60 mV, the channel spent longer time at closed state, but the probability of staying in the long-lasting closed state decreased when the applied PD reached 80 mV. The same response observed when poly(T) was introduced. However, poly(G) caused no significant effect on the channel mean closed time. According to the results, the best differentiation between poly(T), poly(C) and poly(G) is fulfilled when translocation is studied at 60 mV (Figure 3b). Furthermore, based on the δt value obtained for time gap between events, it was clear that in the presence of poly(C) and poly(G), elapsed time decreased as the PD increased, while it was increased when poly(T) was introduced (Figure 4).

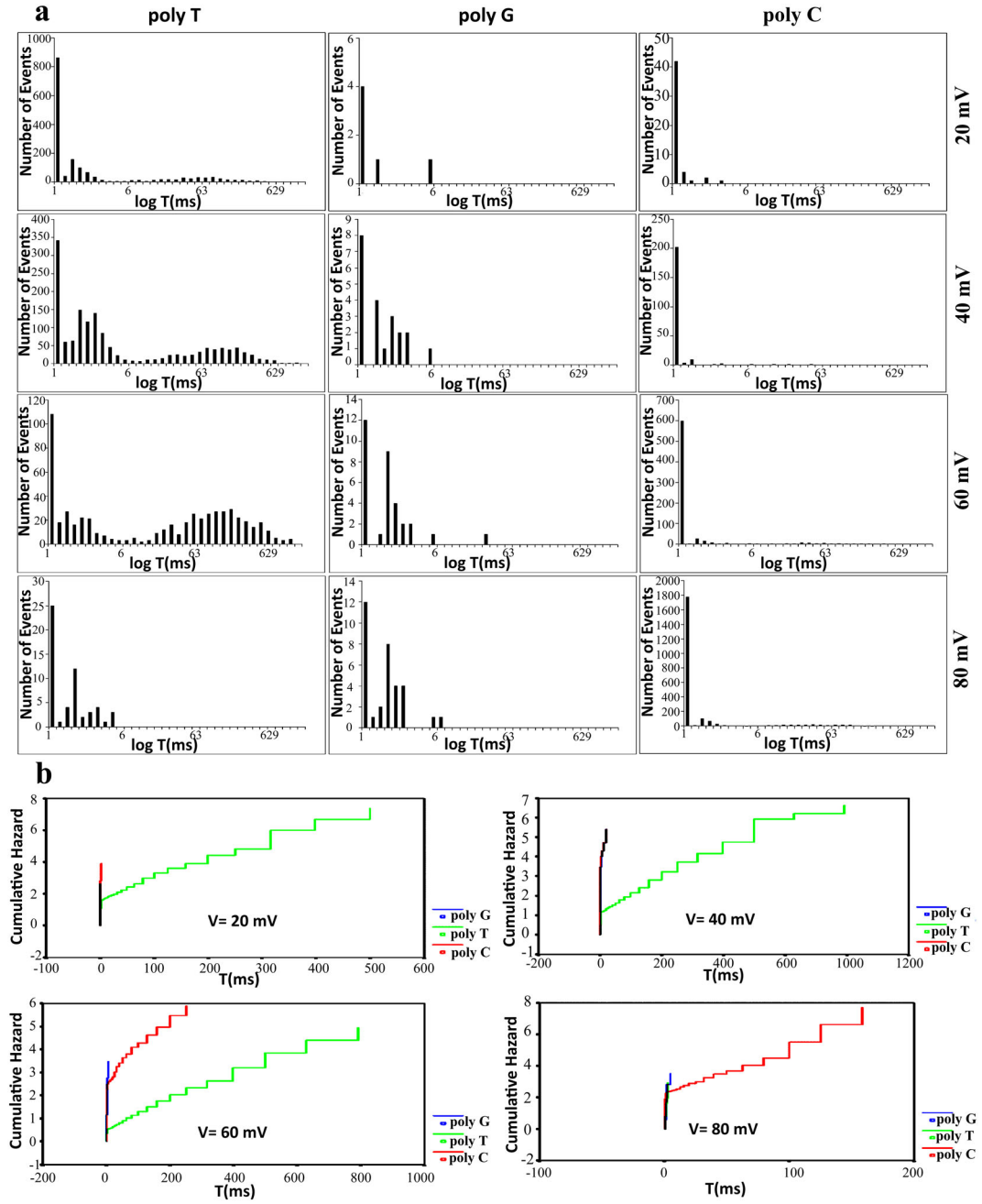

Figure 3. OmpF channel mean closed time in the presence and absence of poly(C), poly(G) and poly(T). The channel mean closed time did not change in the presence of poly(C) at different PDs. However, in the presence of poly(G), it increased as a function of the applied PD. In the presence of poly(T), the mean closed time was significantly increased and led to the formation of long-lived closed states at higher PDs (a). The result of Hazard function analysis is shown against time indicating the significant differentiation at 60 mV (b).

Two different patterns of events monitored in the presence of poly (T) compared with poly(G) and poly(C). The number of events increased in the presence of poly(C) and poly(G) as PDs increased, while it was opposite in the presence of poly(T).

Effects of polynucleotides on OmpF voltage sensitivity

Voltage sensitivity of the OmpF channel was mainly affected at negative polarities in the presence of different polynucleotides (Figure 5). OmpF channel complete closure occurred at about ±160–180 mV, and there has been rarely any complete closure occurring at lower PDs. Introduction of poly(C) to the *cis* side did not affect on the voltage sensitivity at positive polarities, while at negative polarities, there was a complete closure occurring at PDs as high as −160–180 mV. However, there were occasions when sudden, complete closure observed at lower PDs of 60 mV. The channel in monomeric, dimeric and trimeric states at different PDs showed a linear Ohmic behavior (Figure 5). Voltage sensitivity of the channel was decreased in the presence of poly(G) so that complete closure did not observe frequently even at high positive PDs. However, at negative polarities, complete closure occurred at 100–120 mV too. Poly(T) significantly increased voltage sensitivity of the channel at both positive and negative polarities. The voltage sensitivity of the channel

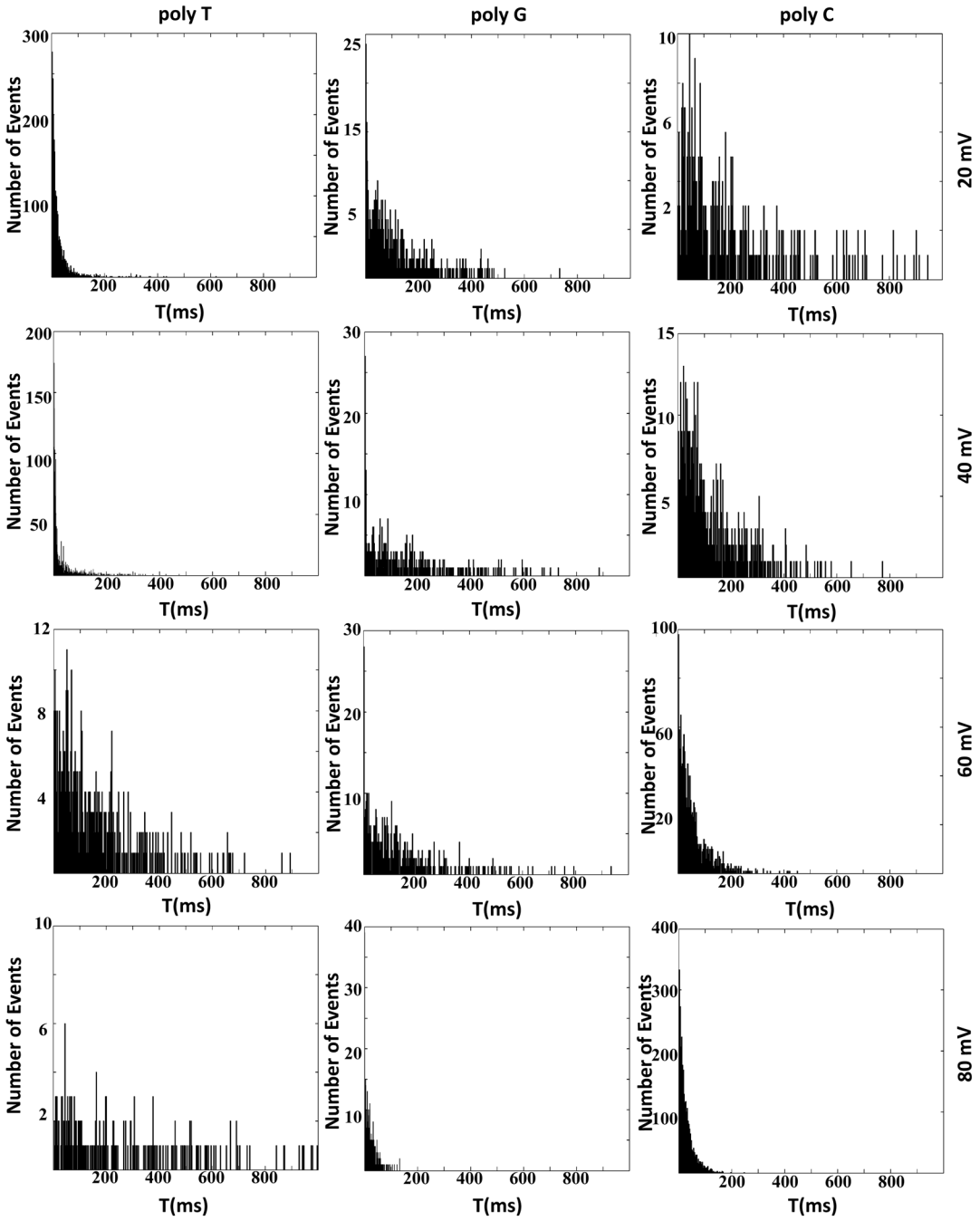

Figure 4. The number of events in OmpF channel as the function of event time length in the presence of poly(C), poly(G) and poly(T) at different PDs. The number of events significantly increased in the presence of poly(T) as PD increased. However, the trend was opposite in the presence of poly(C) and poly(G) so that less events were formed at higher PDs.

increased when it was treated with poly(T) for longer time so that eventually, complete closure of the channel occurred even at PDs as low as −20 and +40 mV (Figure 5).

Nucleotide translocation through OmpF channel

The effects of polynucleotide on channel gating recorded before, one and 30 min after addition showed significant effect as time went by. The conductance of the channel in the presence of poly(G) was 2000 and 2900 pS at negative polarities and 3300 pS at positive polarities only when PD as low as 20 mV was applied. Application of poly(T) also caused a significant decrease in the channel conductance after 15 min so that conductance levels were reduced to 1700 pS at +20 mV, 1500 pS at −20 mV, 1500 and 1600 pS at 40 mV, 1300 and 2900 pS at ±60 mV and eventually 1500 and 3100 pS at −80 mV, while it was 1600 and 2600 pS at +80 mV (Figure 2). Furthermore, while there were initially rarely any gating caused by polynucleotides at positive polarities (Figure 1), after the elapse of 15 min, some gatings were identified at these polarities (Figure 6). However, at negative polarities, the gating initiated at very early time of the presence of polynucleotides and increased over the course of the experiments.

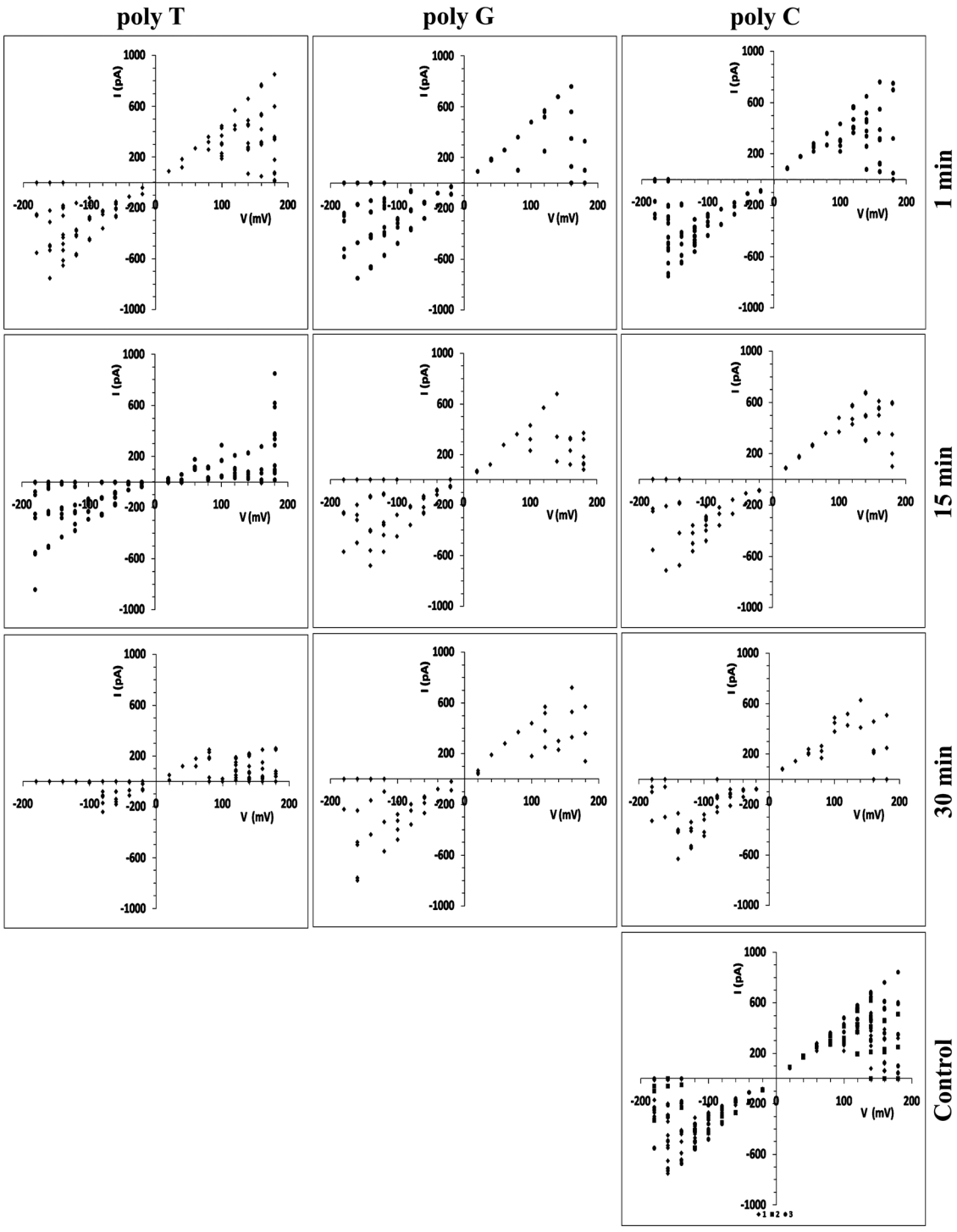

Figure 5. OmpF current voltage curves as a means of showing the ion flux driving force in the presence and absence of poly(C), poly(G) and poly(T) over time. Increased presence of poly(T) in the channel lumen after 15–30 min significantly decreased the current flux even at higher PDs. This trend happened in the presence of poly(G) to a less extent. However, in the presence of poly(C), the pattern was rarely changed, and a conducting path for current carrier ions was available during the course of the experiment. In other words, the trend of blockage caused by polynucleotides was as poly(T) > poly(G) > poly(C).

Interactions of polynucleotides with lining amino acid side chains in OmpF channel lumen

In current simple approach, we used the convenient method to calculate planar polygon area in order to estimate the channel pore area. The center of mass of nucleotides plane (NU) was considered as the center of polygon in vertical direction (SC) relative to main vertical axis of channel (the angles of polygon). The Cα coordinates of residues oriented coplanar with the assumed polygon were considered and based on the Shoelace formula; the area of mentioned

Journal of Molecular Recognition

polygon (PG) was calculated. Accordingly, the relative maximum metric pore free area (PFA) is calculated according to Eqn (1).

$$PFA = PG_{area} - (SC_{area} + NU_{area}) \quad (1)$$

The extent of pore maximum free area available to nucleotides in the vicinity of the constriction zone varied according to the orientation and location of particular nucleotide. The most important data were gathered when the nucleotides considered very close to the constriction zone. The results showed that minimum free area was available in the presence of guanine (475 $Å^2$). There was more free area available in the presence of cytosine (634 $Å^2$) and thiamine (698 $Å^2$; Figure 7a). Furthermore, the lining amino acid side chains and their corresponding amino acids at

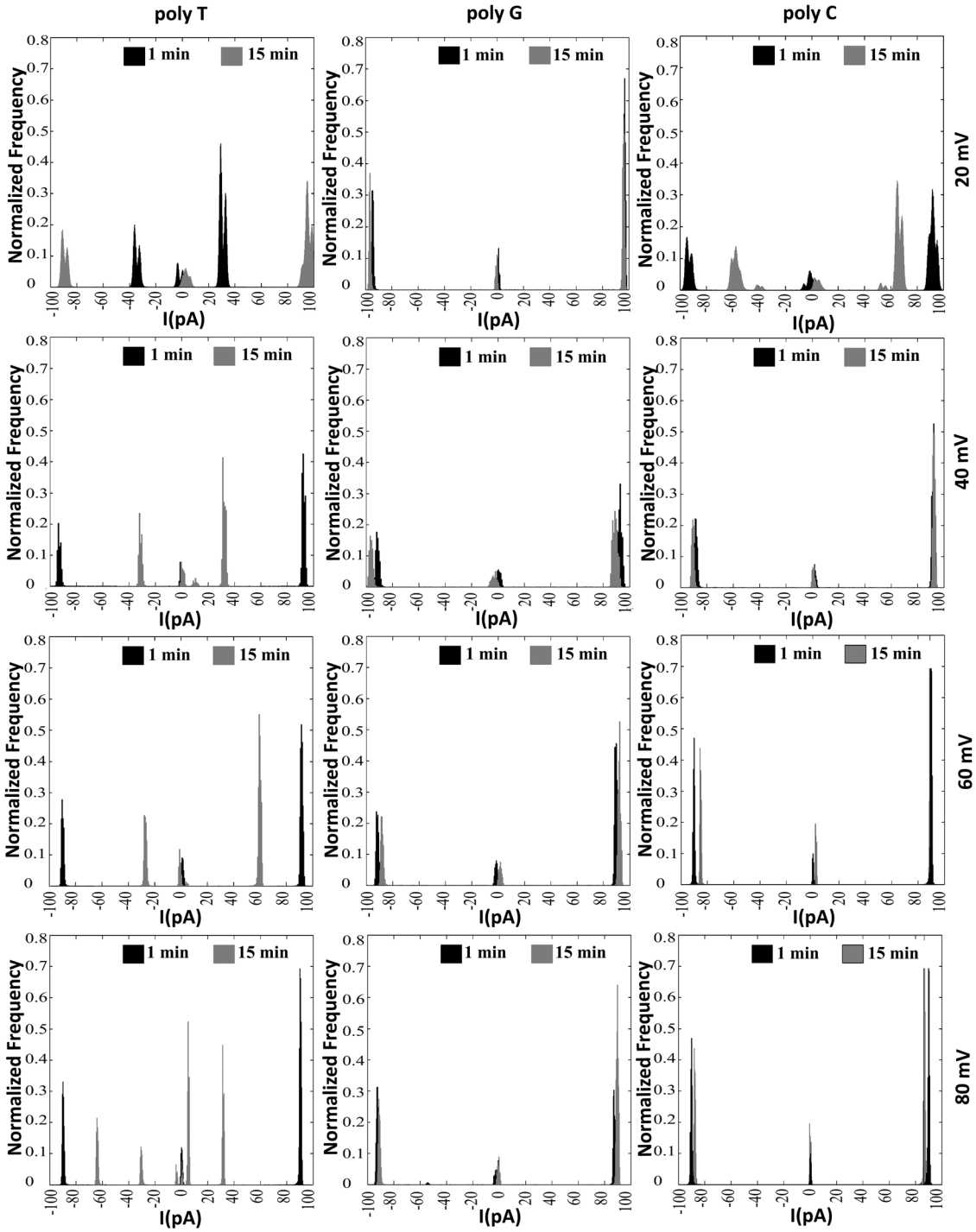

Figure 6. Effects of poly(T), poly(G) and poly(C) on OmpF channel conductance at different PDs 1 and 15 min after introduction of 0.5 nM of polynucleotides. The maximum effects on the decline of conductance were identified in the presence of poly(T), followed by poly(G) and poly(C). Partial or complete blockage of monomers caused by poly(T) in all voltages, but it took place mainly at low PDs by poly(G).

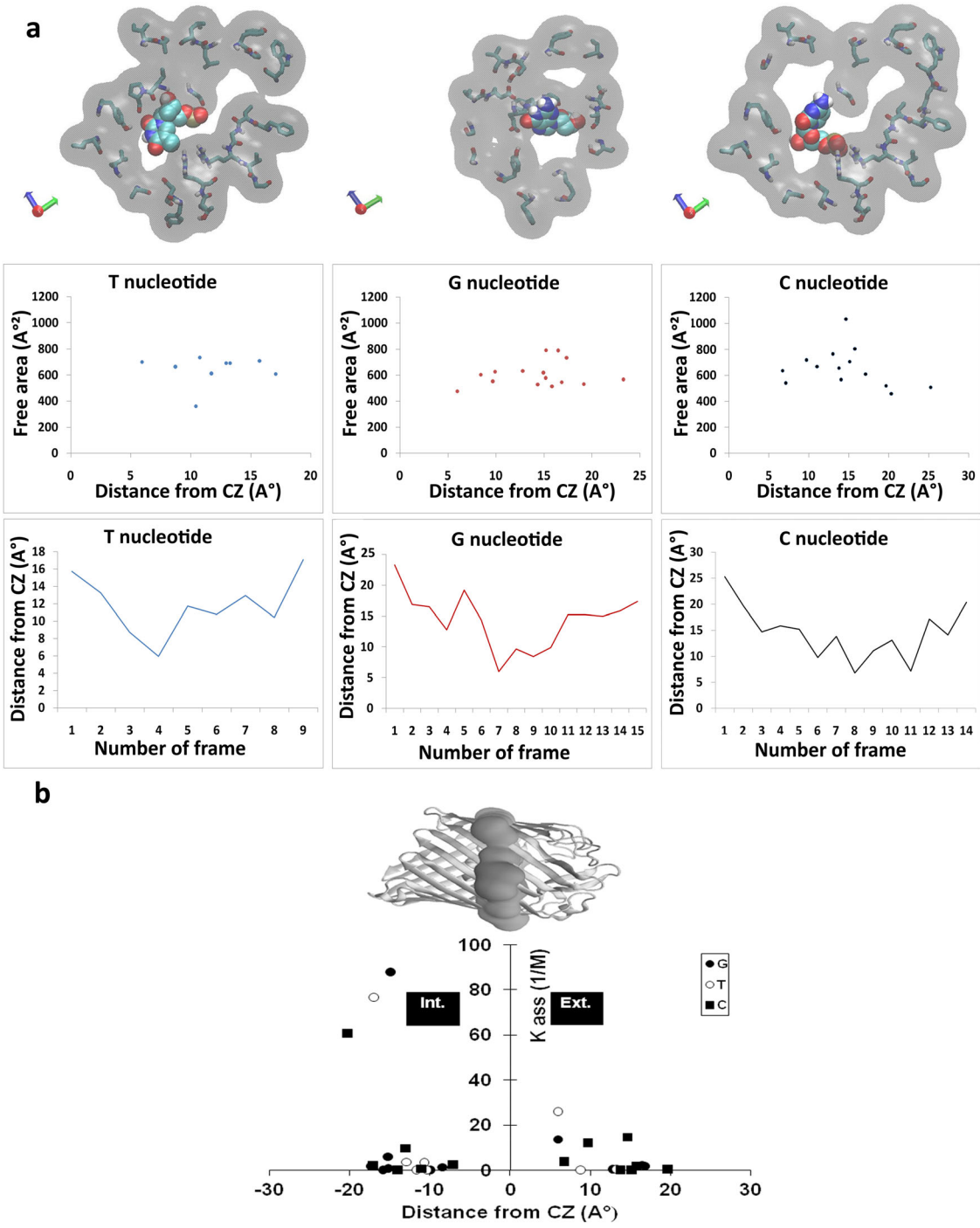

Figure 7. PFA model of OmpF porin channel free area. The arrangement of restricting amino acids (top row), calculated free area in the presence of poly(G), poly(C) and poly(T) (middle row) and distance from constriction zone, CZ, (bottom row) is shown. The free area left for three nucleotides, GTP, CTP and TTP, was 475, 634 and 698 Å^2, respectively (a). Binding constants for nucleotides to different parts of OmpF channel lumen. K (ass), along the channel lumen from the extracellular, Ext, towards intracellular, Int, side on either side of constriction zone, Cz, in the presence of guanine, G, thymine, T, and cytosine, C, are shown (b).

the constriction zone and adjacent to the translocating nucleotides were identified, and their possible interactions were evaluated. There were different amino acids interacting with the translocating nucleotides (Table 1). The main interactions were found to be tyrosine, glycine and aspartic acid that slowed down the translocation. Furthermore, other amino acids, valine and phenylalanine, specifically interacted with cytosine and guanine, and leucine specifically interacted with thymine and guanine that only affected on the flux of corresponding polynucleotides. Another important fact discovered here was the presence of the hydrophobic groups of glycine, alanine, and tyrosine that make a slippery path for all three nucleotides. The interactions set between nucleotides and

Journal of Molecular Recognition

Table 1. Type and number of interacting amino acids with nucleotides at the constriction zone

Nucleotide	G	R	S	D	Y	N	A	L	K	T	F	V
T	4	3	1	2	6	3	1	1	1	2	—	—
C	2	1	1	3	5	1	3	1	1	3	1	2
G	2	2	1	4	5	1	3	—	1	2	1	2

channel lining groups were calculated by LIGPLOT software at various frames. For this purpose, the analysis was conducted on one frame chosen from outer opening, two frames from constriction zone and one frame from internal opening of the channel (Table 2). There are less hydrophobic interactions at either openings of the channel than the constriction zone. On the other hand, maximum hydrogen bonds form at the constriction zone. The maximum free energy of binding exists between guanine and cytosine nucleotides and lining amino acid side chains in the constriction zone. The free energy of binding increases as the nucleotides reach constriction zone and decreases after they pass it. The highest free energy of binding was identified for guanine. Maximum binding constant, K (ass), was obtained when it was calculated for each frame using a free energy equation, $\Delta G = -RT\ln K$, at 298 K (Figure 7b). The calculation showed minimum binding constant for guanine at the constriction zone and maximum values for cytosine and thymine. On the contrary, the binding energy at the external opening of the channel was higher for cytosine and thymine than guanine.

DISCUSSION

Aiming to use OmpF porin nanochannels, as a mean to sequence nucleic acids, translocation of polynucleotides through channel was studied in real time. Different effects of polynucleotides poly(T), poly(G) and poly(C) on channel conductance, blockage, gating pattern, voltage sensitivity, mean closed time and diffusion rate were studied both experimentally and theoretically. It was found that the channel conductance was most affected by poly(T) that obstructed the conducting path and reduced the conductance to about 360 pS. Different from poly(T), poly(C) caused fast flickering at PDs ranging from 20 to 80 mV. This showed certain structural and/or electrostatic compatibility between polynucleotides and channel lumenal groups. Poly(G) acted completely different from poly(T) and poly(C) and caused no effects on conductance or voltage sensitivity. Although poly (G) lowered the channel conductance mainly at negative polarities, the significant decrease was monitored at 20 mV. This fact once more approved the involvement of the channel conformation on the unique signature that each of the applied polynucleotides created.

The results well supported the experimental data and showed that the decrease in the current flow in the presence of thymine, cytosine and guanine was consistent with the less available free area they caused. The least free area was available in the presence of thymine, and this was why most fast flickering caused by this polynucleotide. The binding energy and interactions involved between polynucleotides and lining groups in the channel lumen well represented the speed of movement of polynucleotide through the channel and showed that the higher mean closed time caused by thymine was because of longer residence time of this polynucleotide in the channel constriction zone. The binding affinity of other nucleotides to the entrance of the channel and the hydrophobic interactions identified was consistent with their lower effects on gating and voltage sensitivity.

The polynucleotides used here consisted of ten nucleotides that were not large enough to form a globular structure. Thus, they were linearly inserted into the channel lumen and obstructed the conduction path at the constriction zone. Once polynucleotide reached the eyelet area, some back and forth movements occurred. The flexibility of the channel also played a major role at this stage easing the translocation. The interaction between the channel lining amino acid side chains pointing into the channel lumen and moving polynucleotides varies according to the size, charge and hydration state of nucleotides in strands. Thus, as the polynucleotides get into certain position next to the constriction zone, the frequency of gating and fast flickering was increased. This is why various polynucleotides caused different effects on the gating and conductance of the channel.

Following the introduction of polynucleotides, the main effects were monitored when negative PDs were applied to the *trans* side. The effect initiated by fast flickering at negative polarity with

Table 2. Interactions set between translocating nucleotides and channel lining groups

Nucleotide	Interactions	Ext	Cz 1	Cz 2	Int
G	Number of hydrophobic interactions	4	1	1	3
	Number of hydrogen bonding	3	6	6	5
	Bonding free energy (kcal)	−8.34	−9.4	−9.42	−7.88
C	Number of hydrophobic interactions	3	0	2	5
	Number of hydrogen bonding	1	5	3	2
	Bonding free energy (kcal)	−4.39	−5.22	−6.69	−4.97
T	Number of hydrophobic interactions	4	0	1	4
	Number of hydrogen bonding	2	6	7	2
	Bonding free energy (kcal)	−4.71	−6.64	−4.15	−6.68

The type and number of interactions were calculated by LIGPLOT software at frames representing constriction zone, outer and inner opening area. The frames taken from external, Ext, internal, Int, and constriction zones, Cz1 and Cz2, are shown.

no gating at the opposite polarity. However, at longer time that led further diffusion of polynucleotides, it came the time when fast flickering occurred at opposite polarity, too. We believe that at the early stage of experiments, the nucleotides only existed in the *cis* side and obstructed the conducting path, creating fast flickering of the ion current. Later on when the polynucleotides passed through the pore, they were able to affect on the current flux in the opposite direction. Thus, they now obstructed the cations flowing from the *trans* side toward *cis* at opposite polarity and caused fast flickering at positive polarity applied to the *trans* side. During the process mentioned in the preceding texts, there were occasions when the polynucleotides stuck in the constriction zone causing complete closure of the monomer. This unusual activity was manifested several times at low PDs where the channel at normal condition stayed in fully open state, and no short life gating occurred. Our results showed occasions that when one or two monomers were completely closed, the third one was partially blocked by polynucleotides, and as a result, fast flickering occurred.

The mechanism(s) involved in the translocation of polynucleotides presented here can be explained by the aspects considered by Sing PR *et al*. (Singh *et al*., 2012), who reported the interaction, binding means and electrical driving forces on the translocating peptide through single nanochannel of *Nocardia farcinica* at different voltages. Accordingly, the least binding and translocation hindering is caused by poly(T) followed by poly(G) and then poly(C). Because at lower voltages, less events are manifested for poly(T), and thus, less binding affinity and/or amino acid side chains hindering effects are involved. However, when high PDs are applied, the poly(T)'s are forced into constriction zone of the channel, and thus, because of the obstruction caused by the translocating poly(T)s, more events are manifested. On the other hand, poly(G) and poly(C) interacted with the channel causing a great deal of events at low PDs that were declined when they were pushed away by higher PDs. The polarity of the applied voltage played a significant role too so that when the *cis* side was negative with respect to the *trans* side, more obstructions were caused. Thus, in the presence of poly(T), poly(G) and poly (C), the channel was transiently obstructed and complete halt of current flux occurred at −20, −100 and −120 mV, respectively. The possible binding or hindering means were then overcome at higher PDs. This was when the polynucleotide was dragged out through the pore, and thus, clear constriction zone and fully conductive monomers, dimers and trimmers were monitored. The channel global conformation was affected by the applied PD; thus, at higher PDs, 60 and 80 mV, compared with 20 and 40 mV, the higher PD kept the channel in closed status for longer time. Thus, at higher PDs in the presence of polynucleotides, high frequency gating was caused by more energetic ions that were trying to use any short time available path. On the other hand, the obstructed path by polynucleotide was affected because of flexibility of channel, and a transient short-lived conducting path was resulted. The voltage sensitivity of the channel was impaired by the presence of the polynucleotide, either because of the interaction of strands with voltage sensitive gate or simply because of obstructing the current path that mistakenly may be considered as closure occurring because of changes in the conformation. The OmpF channel conformation switch to closed state at higher PDs, thus, it seems that the polynucleotide induces the formation of a slippery path in the channel to facilitate its translocation. In other words, we are witnessing what that happens in LamB porin where channel conformation is changed in a way that a facilitating slippery path is formed by the translocating sugar whose size is much bigger than the channel vestibule (Jap and Walian, 1995).

Introducing polynucleotides to one side provided the possibility of monitoring their obstruction effects on the channel current flux when the translocated ones were pushed back at opposite polarities. As the concentration of polynucleotides was much higher in the *cis* than *trans* side, and the number of translocating polynucleotide was very low, one would not expect to reach equilibrium within the time course of the experiments. Further, we preferred not to use stirrer in the chamber to avoid membrane disruption; thus, the equilibrium in the two compartments was not reached even after 30 min. We have tried to address the translocation of polynucleotides through the channel; however, we could not expect it to occur with no driving force applied. Thus, we had to apply alternate changes in the polarity that distorted possible transient equilibrium reached at each stage of the experiment. However, the system was gradually reached more equilibrated stages because of presence of polynucleotides in both sides of the constriction zone. Thus, a short life equilibrium was established at the nanoenvironment in the vicinity of the constriction zone. This was manifested as a gradual decline in the current flux at opposite polarities over time and indicated the presence of nucleotides in the *trans* side and approved their translocation to some extent. There were two different patterns of events monitored in the presence of poly(T) compared with poly(G) and poly(C). In the former group, the number of events was increased as a function of the increased PD. However, the opposite pattern was recognized in the latter group. This might show different affinity of the constriction zone of the channel for various polynucleotides so that poly(G) and poly(C) go through some binding activities at low PDs. The obstructions of current flux by these polynucleotides are disrupted by higher PDs, clearing them from constriction zone and causing less events. However, the poly(T)s are not driven to the zone at low PDs, and thus, they are forced into the constriction zone by higher PDs, and as a result, more obstructing events are created.

In conclusion, our results once more approve the involvement of the channel flexibility in the translocation of large molecules that based on the crystal structure of the channel do not fit in the channel, yet alone to pass through. Further, certain PDs cause a unique conformation in the channel and also provide the driving force that favors the translocation of the passing molecule. The results are promising and although are considered as the preliminary results, together with what we published on the translocation of single nucleotides (Nikouei and Mobasheri, 2007) as well as the theoretical analysis of the current traces (under preparation), shows the great potentials of natural nanopores that makes them the unique mean applicable in nucleic acid sequencing biosensors.

Acknowledgements

The financial support of the University of Tehran is appreciated. The authors wish to thank M. Hadi-Alijanvand for her assistance in statistical analysis of data. The critical revision of manuscript by Cristian Vergallo, University of Salento, Italy, is much appreciated.

Journal of Molecular Recognition

REFERENCES

Bainbridge G, Gokce I, Lakey JH. 1998. Voltage gating is a fundamental feature of porin and toxin beta-barrel membrane channels. *FEBS Lett.* **431**(3): 305–308.

Baslé A, Iyer R, Delcour AH. 2004. Subconductance states in OmpF gating. *Biochim. Biophys. Acta* **1664**(1): 100–107.

Binquan L, Hongbo P, Stas P, Steve R, Gustavo S, Glenn M. 2010. Base-by-base Ratcheting of Single Stranded DNA through a Solid-State Nanopore. *Phys. Rev. Lett.* **104**(23): 238103–238106.

Butler TZ, Gundlach JH, Troll MA. 2008. Determination of RNA orientation during translocation through a biological nanopore. *Biophys. J.* **90**(1): 190–198. DOI: 10.1529/biophysj.105.068957.

Cowan SW, Schirmer T, Rummel G, Steiert M, Ghosh R, Pauptit RA, Jansonius JN, Rosenbusch JP. 1992. Crystal structures explain functional properties of two E. coli porins. *Nature.* **358**(6389): 727–733.

Danelon C, Nestorovich EM, Winterhalter M, Ceccarelli M, Bezrukov SM. 2006. Interaction of zwitterionic penicillins with the OmpF channel facilitates their translocation. *Biophys. J.* **90**(5): 1617–1627.

Delcour AH. 1997. Function and modulation of bacterial porins: insights from electrophysiology. *FEMS Microbiol. Lett.* **151**(2): 115–123.

Derrington IM, Butler TZ, Collins MD, Manrao E, Pavlenok M, Niederweis M, Gundlach JH. 2010. Nanopore DNA sequencing with MspA. *Proc. Natl. Acad. Sci. U. S. A.* **107**(37): 16060–16064. DOI: 10.1073/pnas.1001831107.

Franceschini L, Mikhailova E, Bayley H, Maglia G. 2012. Nucleobase recognition at alkaline pH and apparent pKa of single DNA bases immobilised within a biological nanopore. *Chem. Commun.* **48**(10): 1520–1521. DOI: 10.1039/c1cc16124e.

Garavito RM, Rosenbusch JP. 1980. Three-dimensional crystals of an integral membrane protein: an initial x-ray analysis. *J. Cell Biol.* **86**(1): 327–329.

Heng JB, Ho C, Kim T, Timp R, Aksimentiev A, Grinkova YV, Sligar S, Schulten K, Timp G. 2004. Sizing DNA Using a Nanometer-Diameter Pore. *Biophys. J.*, **87**(4): 2905–2911,

Hille B. 1978. Ionic channels in excitable membranes. Current problems and biophysical approaches. *Biophys. J.* **22**(2): 283–294.

Im W, Roux B. 2002. Ion permeation and selectivity of OmpF porin: a theoretical study based on molecular dynamics, Brownian dynamics, and continuum electrodiffusion theory. *J. Mol. Biol.* **322**(4): 851–869.

Iqbal SM, Akin D, Bashir R. 2007. Solid-state nanopore channels with dna selectivity. *Nat. Nanotechnol.*, **2**(4): 243–248.

Jap BK, Walian PJ. 1995. Gliding through sugar channels: how sweet it is! *Nat. Struct. Mol. Biol.* **5**(1): 6–8. DOI: 10.1038/nsb0198-6.

Karshikoff A, Spassov V, Cowan SW, Ladenstein R, Schirmer T. 1994. Electrostatic properties of two porin channels from Escherichia coli. *J. Mol. Biol.* **240**(4): 372–384.

Kasianowicz JJ, Brandin E, Branton D, Deamer DW. 1996. Characterization of individual polynucleotide molecules using a membrane channel. *Proc. Natl. Acad. Sci. U. S. A.* **93**(24): 13770–13772.

Laun B, Stolovitzky G, Glenn M. 2012. Slowing and controlling the translocation of DNA in a solid-state nanopore. *Nanoscale* **4**(4): 1068–1077. DOI: 10.1039/c1nr11201e.

Lee P-H, Kuo K-L, Chu P-Y, Liu EM, Lin J-H. 2009. SLITHER: a web server for generating contiguous conformations of substrate molecules entering into deep active sites of proteins or migrating through channels in membrane transporters. *Nucleic Acids Res.* **37**: 559–564.

Li J, Stein D, McMullan C, Branton D, Aziz MJ, Golovchenko JA. 2001. Ion beam sculpting at nanometre length scales. *Nature,* **412**(6843): 166–169

Luan BQ, Martyna G, Stolovitzky G. 2011. Characterizing and Controlling the Motion of ssDNA in a Solid-State Nanopore. *Biophys. J.* **101**(9): 2214–2222.

Mach T, Neves P, Spiga E, Weingart H, Winterhalter M, Ruggerone P, Ceccarelli M, Gameiro P. 2008. Facilitated permeation of antibiotics across membrane channels--interaction of the quinolone moxifloxacin with the OmpF channel. *J. Am. Chem. Soc.* **130**(40): 13301–13309. DOI: 10.1021/ja803188c

Marquis H, Ficht TA. 1993. The omp2 gene locus of Brucella abortus encodes two homologous outer membrane proteins with properties characteristic of bacterial porins. *Infect. Immun.* **61**(9): 3785–3790.

Masi M, Pagès JM. 2013. Structure, Function and Regulation of Outer Membrane Proteins Involved in Drug Transport in Enterobactericeae: the OmpF/C - TolC Case. *Open Microbiol. J.* **7**: 22–33. DOI: 10.2174/1874285801307010022

Meni W. 2012. Nanopores: A journey towards DNA sequencing. *Phys. Life Rev.* **9**(2): 125–158. DOI: 10.1016/j.plrev.2012.05.010.

Merchant CA, Healy K, Wanunu M, Ray V, Peterman N, Bartel J, Fischbein MD, Venta K, Luo Z, Johnson AT, Drndić M. 2010. DNA translocation through graphene nanopores. *Nano Lett.* 11; **10**(8): 2915–2921. DOI: 10.1021/nl101046t.

Meyer JR, Dobias DT, Weitz JS, Barrick JE, Quick RT, Lenski RE. 2012. Repeatability and Contingency in the Evolution of a Key Innovation in Lambda Phage. *Science* **335**: 428–432.

Montal M′ Mueller P. 1972. Formation of Bimolecular Membranes from Lipid Monolayers and a Study of Their Electrical Properties. *Proc. Natl. Acad. Sci. U. S. A.* **69**(12): 3561–3566.

Müller DJ, Engel A. 1999. Voltage and pH-induced channel closure of porin OmpF visualized by atomic force microscopy. *J. Mol. Biol.* **285**(4): 1347–1351.

Mussi V, Fanzio P, Repetto L, Firpo G, Scaruffi P, Stigliani S, Tonini GP, Valbusa U. 2010. DNA-functionalized solid state nanopore for biosensing. *Nanotechnology* **21**: 145102–145107. DOI: 10.1088/0957-4484/21/14/145102.

Nestorovich EM, Danelon C, Winterhalter M, Bezrukov SM. 2002. Designed to penetrate: time-resolved interaction of single antibiotic molecules with bacterial pores. *Proc. Natl. Acad. Sci. U. S. A.* **99**(15): 9789–9794

Nestorovich EM, Rostovtseva TK, Bezrukov SM. 2003. Residue ionization and ion transport through OmpF channels. *Biophys. J.* **85**(6): 3718–3729. DOI: 10.1016/S0006-3495(03)74788-2.

Nikaido H. 2003. Molecular basis of bacterial outer membrane permeability revisited. *Microbiol. Mol. Biol. Rev.* **67**(4): 593–656.

Nikouei A, Mobasheri H. 2007. Biophysics of nucleotides interactions with protein nanopores. *Proceedings of the WSEAS Int. Conference on Cellular & Molecular Biology - Biophysics & Bioengineering, Athens, Greece.*

Purnell RF, Schmidt J. 2009. Discrimination of Single Base Substitutions in a DNA Strand Immobilized in a Biological Nanopore. *ACS Nano* **3**(9): 2533–2538. DOI: 10.1021/nn900441x

Ramkumar L, Delcour AH. 1997. Complex Inhibition of OmpF and OmpC Bacterial Porins by Polyamines. *J. Biol. Chem.* **272**(30): 18595–18601.

Robertson KM, Tieleman DP. 2002. Molecular basis of voltage gating of OmpF porin. *Biochem. Cell Biol.* **80**(5): 517–523.

Rostovtseva TK, Nestorovich EM, Bezrukov SM. 2002a. Partitioning of differently sized poly(ethylene glycol)s into OmpF porin. *Biophys. J.* **82**: 160–169.

Rostovtseva TK, Komarov A, Bezrukov SM, Colombini M. 2002b. Dynamics of Nucleotides in VDAC Channels: Structure-Specific Noise Generation. *Biophys. J.* **82**(1): 193–205. DOI: 10.1016/S0006-3495(02)75386-1.

Schirmer T. 1998. General and specific porins from bacterial outer membranes. *J. Struct. Biol.* **121**(2): 101–109.

Singh PR, Bárcena-Uribarri I, Modi N, Kleinekathöfer U, Benz R, Winterhalter M, Mahendran KR. 2012. Pulling Peptides across Nanochannels: Resolving Peptide Binding and Translocation through the Hetero-oligomeric Channel from Nocardia farcinica. *ACS Nano* **6**(12): 10699–10707.

Soares CM, Björkstén J, Tapia O. 1995. L3 loop-mediated mechanisms of pore closing in porin: a molecular dynamics perturbation approach. *Protein Eng.* **8**(1):5–12

Stoddart D, Heron AJ, Mikhailova E, Maglia G, Bayley H. 2009. Single-nucleotide discrimination in immobilized DNA oligonucleotides with a biological nanopore. *Proc. Natl. Acad. Sci. U. S. A.* **106**(19): 7702–7707. DOI: 10.1073/pnas.0901054106.

Stoddart D, Maglia G, Mikhailova E, Heron AJ, Bayley H. 2010. Multiple Base-Recognition Sites in a Biological Nanopore: Two Heads are Better than One. *Angew. Chem. Int. Ed.* **49**(3): 556–564. DOI: 10.1002/anie.200905483

Storm AJ, Chen JH, Ling H, Zanbergan HW. 2003. Fabrication of solid-state nanopores with single-nanometre precision. *Nat. Mater.* **2**: 537–540. DOI: 10.1038/nmat941

Tanabe M, Nimigean CM, Iverson TM. 2010. Structural basis for solute transport, nucleotide regulation, and immunological recognition of Neisseria meningitidis PorB. *Proc. Natl. Acad. Sci. U. S. A.* **107**(15): 6811–6816. DOI: 10.1073/pnas.0912115107.

Van Gelder P, Saint N, Phale P, Eppens EF, Prilipov A, van Boxtel R, Rosenbusch JP, Tommassen J. 1997. Voltage sensing in the PhoE and OmpF outer membrane porins of Escherichia coli: role of charged residues. *J. Mol. Biol.* **269**(4): 468–472.

Venkatesan BM, Bashir R. 2010. Nanopore sensors for nucleic acid analysis. *Nat. Nanotechnol.* **6**(10):615–624. DOI: 10.1038/nnano.2011.129.

Wang HY, Li Y, Qin LX, Heyman A, Shoseyov O, Willner I, Long YT, Tian H. 2013. Single-molecule DNA detection using a novel SP1. *Chem. Commun.* **49**: 1741–1743. DOI: 10.1039/c3 cc38939a.

Wiese A, Schröder G, Brandenburg K, Hirsch A, Welte W, Seydel U. 1994. Influence of the lipid matrix on incorporation and function of LPS-free porin from Paracoccus denitrificans. *Biochim. Biophys. Acta* **1190**(2): 231–242.

Zhang W, Hou T, Xu X. 2005. New Born radii deriving method for Generalized Born model. *J. Chem. Inf. Model.* **45**(1): 88–93.